Progress in Scale Modeling, an International Journal

Volume 4 | Issue 1 Article 1

2023

Scale Model Experiments of Toxic Gas Production from the Combustion of Polymers when Applied with Different Droplet Sizes of Water Mist

Nicharee Thinnakornsutubutr
Tokyo University of Science, 7721703@ed.tus.ac.jp

Masayuki Mizuno
Tokyo University of Science, mizuno@rs.tus.ac.jp

Kazunori Kuwana
Tokyo University of Science, kuwana@rs.tus.ac.jp

Recommended Citation

Thinnakornsutubutr, Nicharee; Mizuno, Masayuki; and Kuwana, Kazunori (2023) "Scale Model Experiments of Toxic Gas Production from the Combustion of Polymers when Applied with Different Droplet Sizes of Water Mist," *Progress in Scale Modeling, an International Journal*: Vol. 4: Iss. 1, Article 1.
DOI: https://doi.org/10.13023/psmij.2023.04-01-01
Available at: https://uknowledge.uky.edu/psmij/vol4/iss1/1

Scale Model Experiments of Toxic Gas Production from the Combustion of Polymers when Applied with Different Droplet Sizes of Water Mist

Category

Research Article

Abstract

This research experimentally investigated the combustion of polymeric materials with water mist application in an enclosure, with an emphasis on the production of toxic gases. Two different diameters, ~100 and ~260 μm, were tested. The experimental conditions were determined based on Froude similarity laws for low drop Reynolds number conditions. Droplets and polymers' physical and chemical properties influence the burning/extinguishing behavior and toxic-gas evolution. In general, larger droplets can extinguish a fire in a shorter time, and toxic gas concentrations in a test chamber decreased more rapidly. However, the large droplets tended to cause the flame expansion phenomenon for thermoplastics by splashing molten polymer. This flame expansion phenomenon led to a rapid increase in toxic-gas production rate. For a smaller size of water droplets, the formation of a char layer tended to slow down the fire-extinguishing process, which caused continuous CO production.

Keywords

Small-scale tests, Water mist, Froude similarity law, Low drop Reynolds number, Fire toxic gases

Cover Page Footnote

This is a fully-reviewed paper expanded from work that was presented at the 9th International Symposium on Scale Modeling (ISSM9), held in March 2022 in Naples, Italy.

Progress in Scale Modeling, an International Journal, Vol. 4, Issue 1 (2023) Article 04-01-01, pp. 1–12
https://doi.org/10.13023/psmij.2023.04-01-01

Scale model experiments of toxic gas production from the combustion of polymers when applied with different droplet sizes of water mist

Nicharee Thinnakornsutibutr*, Masayuki Mizuno, Kazunori Kuwana

Department of Global Fire Science and Technology, Graduate School of Science and Technology, Tokyo University of Science, 2641 Yamazaki, Noda, Chiba 278-8510, Japan

E-mail addresses: 7721703@ed.tus.ac.jp, mizuno@rs.tus.ac.jp, kuwana@rs.tus.ac.jp

Received November 21, 2022, Accepted February 4, 2023

Abstract

This research experimentally investigated the combustion of polymeric materials with water mist application in an enclosure, with an emphasis on the production of toxic gases. Two different diameters, ~100 and ~260 μm, were tested. The experimental conditions were determined based on Froude similarity laws for low drop Reynolds number conditions. Droplets and polymers' physical and chemical properties influence the burning/extinguishing behavior and toxic-gas evolution. In general, larger droplets can extinguish a fire in a shorter time, and toxic gas concentrations in a test chamber decrease more rapidly. However, the large droplets tended to cause the flame expansion phenomenon for thermoplastics by splashing molten polymer. This flame expansion phenomenon led to a rapid increase in toxic-gas production rate. For a smaller size of water droplets, the formation of a char layer tended to slow down the fire-extinguishing process, which caused continuous CO production.

Keywords: Small-scale tests; Water mist; Froude similarity law; Low drop Reynolds number; Fire toxic gases

Introduction

These days, the use of polymeric materials has been widely established in various products such as automotive, construction, clothing, and packaging industries [1]; the popularity of these materials has increased. Undoubtedly, burning carbon-containing combustible materials can harm human health when they are exposed to "smoke inhalation" [2]. In 2019, a major fire disaster occurred in Kyoto, Japan. More than 70 casualties were found in the Kyoto Animation Studio fire after an arson attack [3, 4]. As gasoline was poured and a blaze was set up near the front door, the flames and smoke instantly traveled to every floor of the three-story building. The massive amount of smoke production can slow down and block occupants. Consequently, most of them could not have enough time to escape from the smoke-filling building. In particular, inhaling highly toxic gases mainly affects the respiratory system through physiologic malfunction. According to this catastrophe, it was reported that 28 people from the 33 total fatalities were lifeless due to toxic gas inhalation [5]. Thus, the analysis of toxic-gas production during fire accidents must be seriously considered.

Water mist protection is one of the recent technologies for organizations where water damage is a significant issue. Also, it can be used instead of several types of fire extinguishment agents with its advantages: non-conductivity, less damage to property than sprinklers, and environmental friendliness. Fires can be extinguished or reduced in size with two dominant physical mechanisms of water mist droplets, wetting and cooling fuel surfaces and oxygen displacement due to evaporation of water mist [6, 7]. Many researchers studied various factors such as water droplet size and distribution, water flux density, spray flow rate, water droplet velocity, and the operating pressure at nozzles, which can enhance the fire-suppression efficiency of water mist systems. The most important variable for fire extinguishment was found to be the size of water droplets [8].

On the other hand, few studies have been conducted on the influence of water spray on toxic gas generation from burning materials. The effects of toxic gases produced during water mist discharging mainly concern behavioral incapacitation, injury, and death during fires

Progress in Scale Modeling
AN INTERNATIONAL JOURNAL
https://uknowledge.uky.edu/psmij/

Table 1. Similarity rules for the interaction between water mist and fire.

Scaling parameters	Froude similarity laws
Temperature, T [K]	$\frac{T}{T'} = \left(\frac{L}{L'}\right)^0$
Gas concentration, C [mol/m^3]	$\frac{C}{C'} = \left(\frac{L}{L'}\right)^0$
Heat release rate, Q [kW]	$\frac{Q}{Q'} = \left(\frac{L}{L'}\right)^{\frac{5}{2}}$
Water flow rate, V [L/min]	$\frac{V}{V'} = \left(\frac{L}{L'}\right)^{\frac{5}{2}}$
Water flux density, J [L/m^2·min]	$\frac{J}{J'} = \left(\frac{L}{L'}\right)^{\frac{1}{2}}$
Water droplet diameter, d [μm]	$\frac{d}{d'} = \left(\frac{L}{L'}\right)^{\frac{1}{4}}$

[9–11].

Previously, Hietaniemi et al. conducted a series of experiments to determine the burning characteristics and the yield of produced toxic gases with and without the suppression of water spray on polypropylene (PP) and nylon-6,6 combustion in a control-ventilated cone calorimeter [12]. The results indicated that the yields of CO and HCN produced from the combustion of polymers with water spray discharge were twice as large as those without it, demonstrating that the suppression by water spray could cause several kinds of fire toxic-gas production.

Shelley et al. analyzed the tenability of television fires in a sprinkler-protected compartment [13]. The real-scale experiment was conducted with test samples: televisions composed of polystyrene (PS) with flame retardant. Analysis of produced gases, such as CO and CO_2, was carried out along with the compartment temperature and the fuel's mass loss rate. The results showed that if the occupants had relied on sprinkler activation to notify them of a fire, their available safe escape time would have been limited. Water-based fire suppressions most likely led to decreased tenability by disturbing the hot, toxic smoke layer, allowing it to reach a lower part of the compartment. These previous studies demonstrate that understanding toxic-gas production with water mist is still not comprehended.

Heskestad [14] derived scaling laws of the interaction between water droplets and flames. Later, Jayaweera and Yu [15] and Yu [16] derived modified scaling laws for low drop Reynolds number conditions. Both studies extended the standard Froude-number scaling laws to consider the dynamic interaction of water drops with convective flows and drop evaporation. The quasi-steady drop vaporization with the d^2 law is assumed in deriving the scaling laws.

This study reports the results of scale-model experiments of toxic-gas production from the burning polymers when applied with water mist. In designing the experiments, a prototype fire is specified: an upholstered, small piece of furniture catches fire inside a compartment, and a water mist is applied at the initial stage of the fire. Because the drop Reynolds number of water mist (mean diameter less than 1 mm) is small, the scaling laws proposed by Jayaweera and Yu [15] and Yu [16] are adopted in this study.

The objective of the present study is to understand the influences of water mist and polymer properties on burning and extinguishing behaviors with an emphasis on the production of toxic gases in the enclosure.

Experimental setup

Scaling considerations

Since our prototype scenario reflects early fire detection and subsequent water-mist application, the heat release rate at the moment of water-mist activation is set to 100 kW or less. Note that the maximum heat release rate can achieve roughly 300–1000 kW [17] when a small, upholstered chair is burned without any extinguishing efforts.

The NFPA 750 standard [18] defines the mean droplet diameter of water mist as 100–1000 μm, and smaller droplets are considered more effective for fire extinguishment. The size of prototype water droplets is thus chosen to be less than 500 μm. The prototype

Table 2. The setup conditions of prototype and scale models.

Scaling parameters	Prototype	Scale models in this study
Compartment height [m]	2.7	0.9
Heat release rate [kW]	< 100	< 10
Water droplet diameter [μm]	< 500	106, 263
Water flux density [L/m²·min]	2.8	1.6

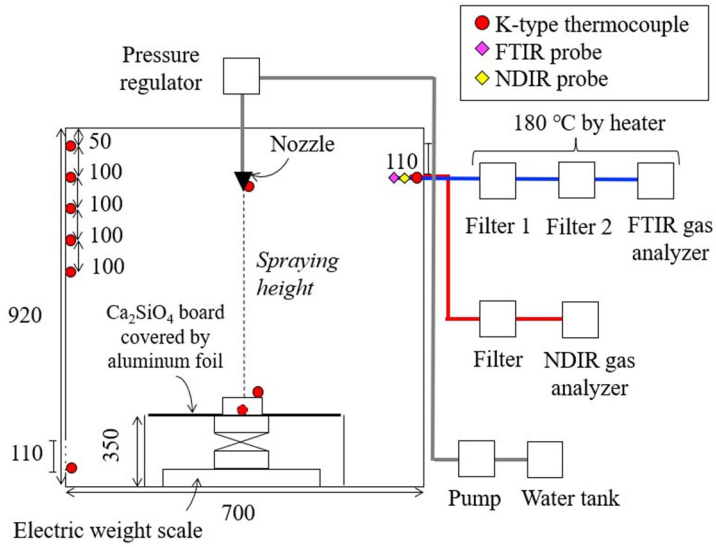

Fig. 1. Schematic diagram of the combustion chamber connected to the test apparatus (unit: mm).

water flux density is set to be 2.8 L/m²·min based on the value of a standard sprinkler [19].

A 1/3 scale-model experiment can be designed by considering the scaling laws shown in Table 1, where L is the characteristic length scale defined as the spraying height between the nozzle and solid fuel top surface. Table 2 summarizes the experimental parameters of the prototype and the scale models used in this study.

Experimental apparatus

The scale-model experiments were conducted in the Fire Research and Test Laboratory, Center for Fire Science and Technology at Tokyo University of Science. Fig. 1 shows the schematic of a 0.70 m × 0.70 m × 0.92 m (height) stainless-steel chamber with four openings on the sides, two near the top for smoke ventilation and two near the bottom for air supply. The combustion chamber was connected to measuring devices and water-spraying equipment. The water mist nozzle was installed at the upper part of the chamber and connected to a high-pressure water pump (Koshin, MS-252CL) through a water pressure regulator, piping, and fittings. The vertical distribution of temperatures was measured by K-type thermocouples with a thin wire (0.32 mm in diameter) installed in the chamber. The thermocouples' response time in the gas phase is approximately 5 s in quiescent air (regardless of convective and radiative heat transfer), which is short enough for our purposes.

The concentrations of CO (in the range of 0–5000 ppm) and CO_2 (0–5%) were measured by a nondispersive infrared (NDIR) gas analyzer (Fuji Electric Co., Ltd), and the concentration of O_2 (0–25%) was measured by a magnetic oxygen analyzer, installed in the NDIR system, with a sampling rate of 1.0 L/min. The concentrations of other low-molecular-weight gases such as NO, NO_2, HF, HCl, acrolein, and formaldehyde were measured by a Fourier transform infrared (FTIR) gas analyzer (Gasmet, DX4000N) with a sampling rate of 4.0 L/min. The concentrations of produced gases were measured near the ceiling because they are expected to be higher than those near the floor and are important safety indices. The temperature and gas concentrations were recorded by a 20-channel data logger (GRAPHTEC: GL820, sampling period: ≥10 ms, and time/div: 1 s).

The test samples in these experiments were timber, polypropylene (PP), polyethylene (PE), polymethylmethacrylate (PMMA), polyurethane foam (PU), and polystyrene foam (PS). The size of the test samples was determined to achieve the heat release rate shown in Table 2. The details of test sample configurations and characteristics are shown in Fig. 2 and Table 3, respectively.

The visual observations of the ignition, fire extinguishing process, and smoke movement were made with video cameras from the combustion chamber's

Table 3. The characteristics of the test sample.

Test sample	Size [m³]	Number of sampes from the top	Total number of samples	Shape
Timbers	0.02×0.02×0.12	3/3/4	10	Crib
PP	0.02×0.02×0.08	3	3	Pieces
PE	0.02×0.02×0.12	3/3/4	10	Crib
PMMA	0.02×0.02×0.12	3/3/4	10	Crib
PU	0.03×0.12×0.12	1/1	2	Bulk
PS	0.02×0.12×0.12	1/1/1	3	Bulk

Table 4. The characteristics of water mist nozzles.

Parameters	Nozzzle 7KB	Nozzle J20
Operating pressure [MPa]	1.0	1.0
Spray flow rate [g/s]	0.388	0.396
Water flux density [L/m²·min]	1.625	1.619
Average mean diameter, D_{10} [μm]	82.8	160.4
Sauter mean diameter, D_{32} [μm]	106.2	262.7

(a) Crib (b) Pieces (c) Bulk

Fig. 2. Test sample configurations.

front, side, and back. The mass-loss rate was measured using a set of electric weight scales under the test sample. The heat release rate ($\dot{Q}$) of the sample before discharging water was calculated from the following equations, where $\dot{m}$ is mass loss rate [kg/s], and ΔH is the heat of combustion [MJ/kg].

$$\dot{Q} = \dot{m} \times \Delta H \quad (1)$$

Before acquiring the data, the gas analyzers were calibrated to maintain the stability of the atmosphere inside the chamber. Each test sample was placed at the center of the combustion chamber below the position of the nozzle. Experiments were conducted more than twice in each condition, and the reproductivity of the results could approximately be confirmed. The sample was ignited using a flammable gel whose primary composition was methanol.

Water was sprayed from the water mist nozzle at a specific time, depending upon the type of the test sample. For timber, PP, PE, and PMMA samples, water was sprayed when the flame achieved a nearly steady state, and the boundary of the smoke and air layers reached approximately 350 and 450 mm from the ceiling. On the other hand, PU and PS foam samples did not produce as thick a smoke layer as the other samples. Therefore, the water mist was discharged as soon as half of the sample's height was burned, at which steady burning was achieved based on the visual observation. Water mist was applied until the fire extinction was achieved. Then, the water pump was deactivated to stop water spraying on the test sample. If the combustion of the test sample was not extinguished within 15 minutes, additional water for fire suppression was applied from the opening to the test sample until the combustion was completely extinguished. The gas analyzers were halted when the concentrations of detected gases declined to normal levels in the atmosphere. In particular, the concentrations of O2 and CO declined to approximately 21% and 0.08 ppm, respectively.

Water mist characteristics

Two sets of full-cone water spray nozzles, called "7KB" and "J20," were selected from the Ikeuchi company. The water droplet characteristics of each nozzle, measured during preliminary experiments, are shown in Table 4. The preliminary experiments were conducted to measure the water flux density of each nozzle without combustion. During the initial tests, the horizontally projected area discharged by water droplets was fixed to 0.01431 m² on the test sample's top surface

$t = 90$s $t = 102$ s $t = 240$ s
Water activated
(a) Nozzle 7KB

$t = 90$s $t = 93$ s $t = 95$ s
Water activated
(b) Nozzle J20

Fig. 3. Timber combustion with water mist by the nozzles (a) 7KB and (b) J20.

$t = 340$s $t = 350$ s $t = 352$ s
Water activated
(a) Nozzle 7KB

$t = 290$s $t = 300$ s $t = 301$ s
Water activated
(b) Nozzle J20

Fig. 4. PP combustion with water mist by the nozzles (a) 7KB and (b) J20.

level. The spraying heights from the nozzle to the solid fuel top surface were regulated at 0.20 m in nozzle 7KB and 0.25 m in nozzle J20 so that the water flux densities are nearly equal to the value shown in Table 2. The Sauter mean droplet diameters of water spraying on the same horizontally projected area with the nozzles 7KB and J20 were 106.2 and 262.7 μm, respectively.

Results and discussion

Observations

During combustion

Timbers burning in the combustion chamber are shown in Fig. 3. It can be observed that after discharging the water mist from nozzles 7KB (Fig. 3(a)), the flame gradually decreased its size and was eventually extinguished. For nozzle J20 (Fig. 3(b)), on the other hand, it took a shorter time to extinguish the fire. PMMA samples showed similar burning and extinguishing characteristics to timbers. PS samples did not have self-sustaining properties in combustion, and only some parts of the samples that were close to the flames from the methanol gel spots burned while melting. The different extinguishing characteristics (time to extinguish) between the two nozzles were similar to those of timber and PMMA.

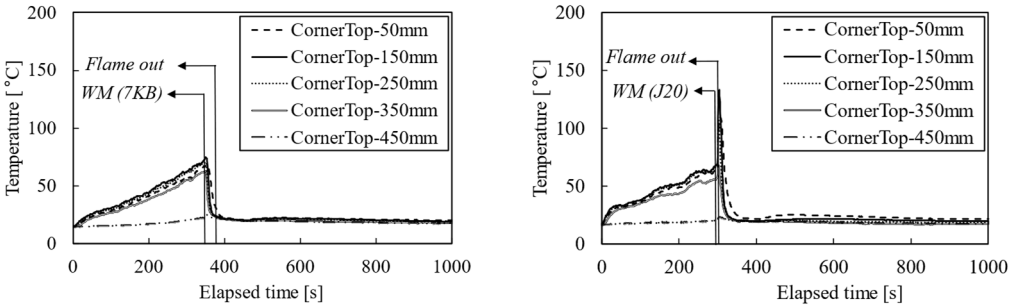

(a) Nozzle 7KB (b) Nozzle J20

Fig. 5. Temperatures in the case of PP with the injection of water mist.

$t = 90$s $t = 101$ s $t = 102$ s

Water activated

(a) Nozzle 7KB

$t = 90$s $t = 95$ s $t = 96$ s

Water activated

(b) Nozzle J20

Fig. 6. PU combustion with water mist by the nozzles (a) 7KB and (b) J20.

While PE and PP followed similar processes to Fig. 3 when extinguished with nozzle 7KB, they showed different behaviors when extinguished with nozzle J20. The flaring-up of the flame was observed after the activation of the water mist, as shown in Fig. 4(b) at $t = 300$ s and 301 s. Immediately after the water-mist activation, the flame height momentarily increased (Fig. 4(b) at $t = 300$ s). Then, an explosive expansion of the flame followed; increase in volumetric expansion with the flame, and then the flame instantaneously disappeared (Fig. 4(b) at $t = 301$ s). The observations are consistent with local temperatures measured near the chamber corner by five thermocouples shown in Fig. 5. When the water mist was discharged from nozzle J20, the local temperatures suddenly increased from 25 °C to 140 °C (Fig. 5(b)) because the flame expanded its volume and approached the thermocouples. Large droplets from nozzle J20 reached the hot liquified fuel surface and splashed the molten polymer, accelerating the gasification of the splashed fuel, and consequently, the flame height increased. The water droplets then quickly evaporated and caused a sudden volumetric expansion of the flame, increasing the flame volume.

The PU sample also showed a flame-expansion phenomenon. Although the flame height decreased immediately after the water mist was activated, an explosive expansion occurred within a few seconds, as shown in Fig. 6(b) at $t = 95$ s and 96 s. Unlike PP and PE, splashing by water mist and rapid increase of the flame height were not observed. The burning surface of the PU sample was highly viscous brownish substances, which did not splash upon water-droplet hitting on the surface. Nevertheless, water droplets rapidly evaporated and caused flame expansion. On the contrary, water droplets from the nozzle 7KB were so small that they evaporated before and during penetrating the flame, not contributing to flame expansion.

A similar flame-expansion phenomenon was observed during water-mist suppression of a cooking oil fire reported by Qin et al. [20], who also reported a similar trend of temperature evolution. The present results show that, similar to liquid fuels, suppressing a thermoplastic-polymer fire with water mist may cause an increase in visible flame size.

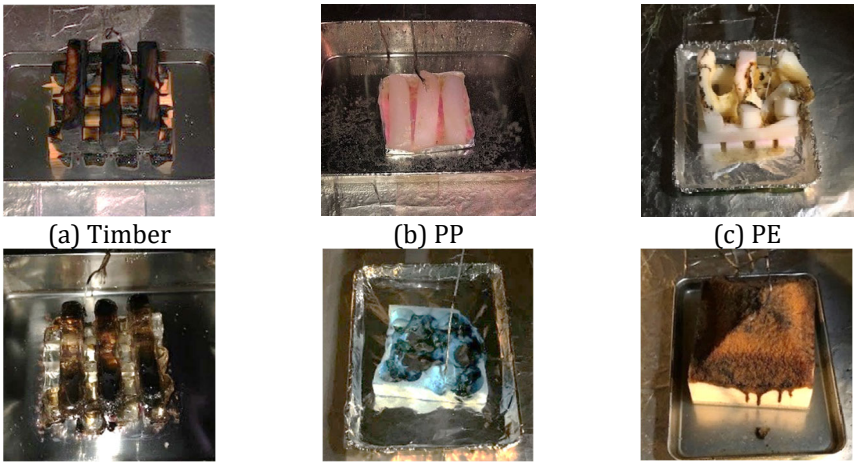

(a) Timber (b) PP (c) PE

(d) PMMA (e) PS (f) PU

Fig. 7. Test samples after the combustion.

Table 5. Fire performance of polymers burning.

Test sample	Weight of test sample [g]		HRR [kW]	Fire extinguishing time [s]	
	Before	After		Nozzle 7KB	Nozzle J20
Timber	190.7	177.3	6.0–8.0	191	18
PP	107.7	106.6	~5.0	5	2
PE	489.1	474.2	2.0–4.0	Not extinguished	3
PMMA	589.5	547.8	8.0	16	2
PU	51.1	38.5	6.0–8.0	10	1
PS	44.5	44.5	2.0	70	5

Samples after the combustion

The photographs of each test sample after the combustion are shown in Fig. 7. The surface layers of black and brown char were observed in timber and PU in Figs. 7(a) and 7(f), respectively. PS foam was also black char-forming at the melted surface without self-sustaining combustion as seen in Fig. 7(e).

PP, PE, and PMMA (Figs. 7(b), (c), and (d), respectively) are thermoplastics. Upon heating, PMMA softens owing to its decomposition into monomers, while PP and PE melt to form liquid layers on their surfaces. Plastic chains behave like a liquid state and finally burn without a charring state, making the burning characteristics different from the other thermosetting test samples (foam-typed PU and PS). PMMA sample was the only thermoplastic test sample that produced a black carbonaceous material on its surface, as shown in Fig. 7(d).

Extinction limit

Table 5 presents the results of the time to extinction by nozzles 7KB and J20. The combustion of the polymers took 10 to 191 s to be completely extinguished with water mist discharged by nozzle 7KB. PE was an exception that could not be extinguished with the small-sized water droplets, although the flame was controlled to a smaller size. On the other hand, with nozzle J20, all test samples could be successfully extinguished in a shorter time compared to nozzle 7KB. For instance, PP and PE took only 2–3 s to extinguish completely with nozzle J20, confirming the significant influence of droplet size. Small droplets quickly evaporate and do not reach the fuel surface for direct cooling. While direct cooling of the combustible material is the primary extinguishing mechanism for larger droplets (J20), the increased water vapor concentration from quick vaporization promotes the smothering effect for smaller droplets (7KB).

Focusing on the suppression by nozzle 7KB, timber combustion took 191 s to be extinguished, which was longer than the other test samples due to its char-forming nature, which can be confirmed in Fig. 7(a). Direct heat transfer from the flame was inhibited to the timber due to the insulating char layer [21], limiting the cooling of the timber; water mist droplets were blocked from reaching the pyrolysis region beneath the char layer. The same mechanism applies to the combustion of PU, contributing to the 10-s extinction time. Because of the aromatic groups in the main chain (diisocyanate group), PU generated the brownish sticky substance on the sample's surface (Fig. 7(f)), which can slow the heat transfer between the gaseous and condensed phases.

In the case of PMMA, the combustion was extinguished with water spray in 16 s. Dissimilar to char-forming timber, the substance formed on the surface of PMMA is not a carbonization layer. It could not hinder

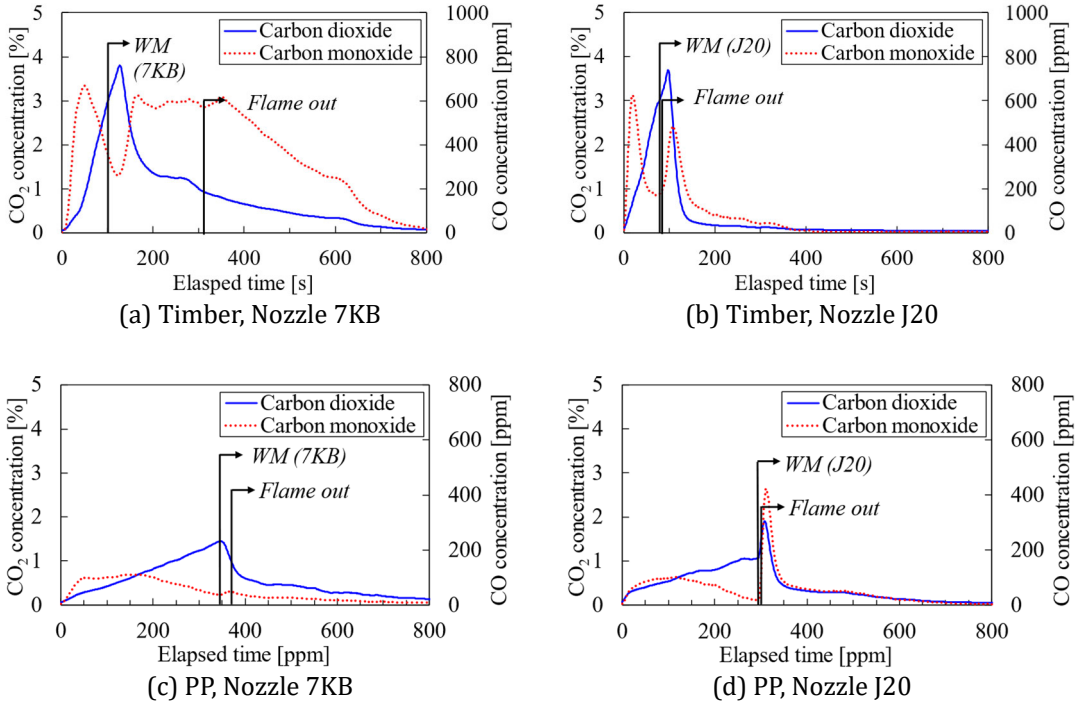

(a) Timber, Nozzle 7KB (b) Timber, Nozzle J20

(c) PP, Nozzle 7KB (d) PP, Nozzle J20

Fig. 8. The concentrations of CO and CO_2.

the heat transfer in the condensed phase. Other thermoplastics, PE and PP, tended to be flammable when heated beyond their melting points, so it is hard to extinguish those samples in a short time. The water flux density, which is affected by the droplet diameter of the water mist, served as the main parameter to describe the extinction limit of both thermoplastics due to the re-ignition of the melt pool. The combustion of PE cannot be extinguished with the application of small-size water droplets owing to the lack of water flux density at the surface, so additional water suppression from the opening was necessary for the extinguishment.

Toxic gas production

CO and CO_2 concentrations

Figs. 8(a) and 8(b) show the evolutions of CO and CO_2 concentrations from timber combustion, measured by a gas analyzer inside the top opening of the chamber. After ignition, a smoke layer formed beneath the ceiling, and the CO concentration increased and peaked at approximately 600 ppm within 1 min, indicating that timber combustion immediately after ignition is incomplete and produces toxic gases at high levels. In our experiments, methanol gels were used for ignition. Immediately after ignition, bluish flame characteristics of methanol combustion were observed for about 50 s, after which intense, luminous flames were formed. The formation of CO at the initial stage may be influenced by methanol combustion. Since water mist is activated after the onset of intense sample burning, methanol is expected to have minor influences on the trends of toxic gas concentrations reported below.

At approximately 100 s after ignition, water mist was discharged from the nozzle near the ceiling, penetrating the smoke layer accumulated beneath the ceiling. Elevated CO concentrations were detected after applying water spray.

The CO production caused by the water mist can be connected to the following reaction between water vapor and solid carbon such as char and soot [22]:

$$C(s) + H_2O(g) \rightarrow CO + H_2 \quad (2)$$

In addition, the following reaction between hydrocarbon and water enhances CO production [23], where $m + m' = n$.

$$C_nH_{2n+2} + m'H_2O \rightarrow C_mH_{2m+2} + m'CO + 2m'H_2 \quad (3)$$

In the timber suppression, the reduction rates of CO and CO_2 to negligible levels differed between the two nozzles. It took about 320 s for the CO concentration to decrease to nearly zero after water was discharged by nozzle J20. In the case of nozzle 7KB, on the other hand, the concentrations of CO took about 700 s to reduce to negligible levels because the fire was not readily extinguished. Although the flame appears to be put out about 200 s after water discharge, smoldering combustion continued, producing CO. PS and PMMA show similar CO and CO_2 evolution to timber combustion. PMMA is not char-forming material but produces a carbonaceous substance on its surface (Fig. 7(d)), which may contribute to producing CO by a similar reaction to (2).

In the case of PP combustion, a substantial difference between the two nozzles was observed at the time of water-mist application. With nozzle J20 (Fig. 8(d)), the

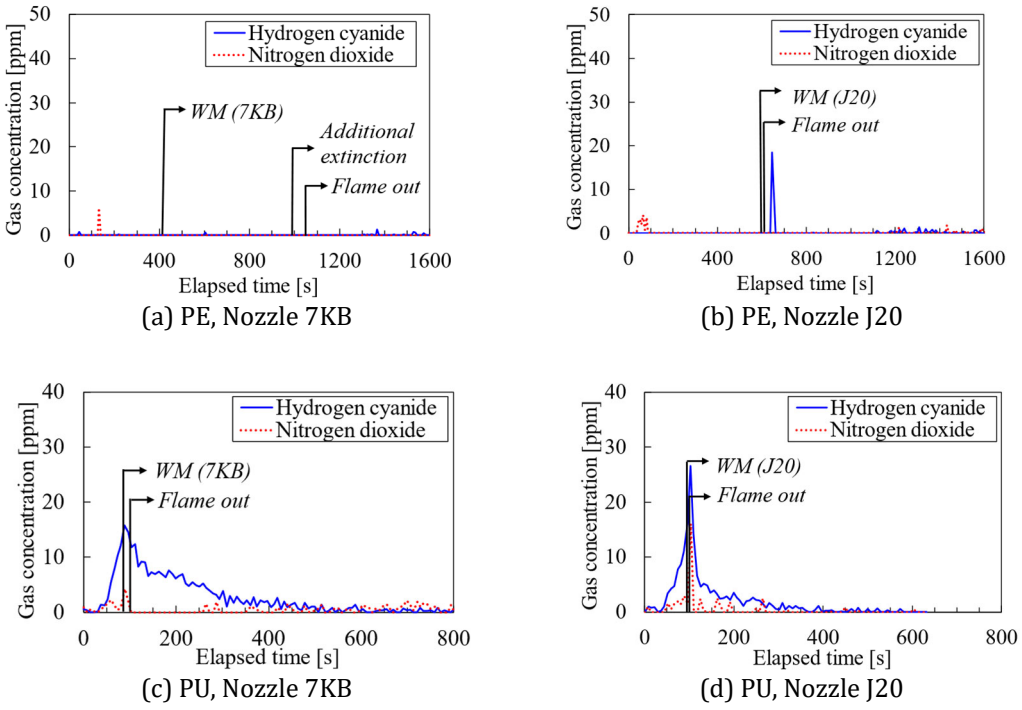

(a) PE, Nozzle 7KB (b) PE, Nozzle J20

(c) PU, Nozzle 7KB (d) PU, Nozzle J20

Fig. 9. The concentrations of HCN.

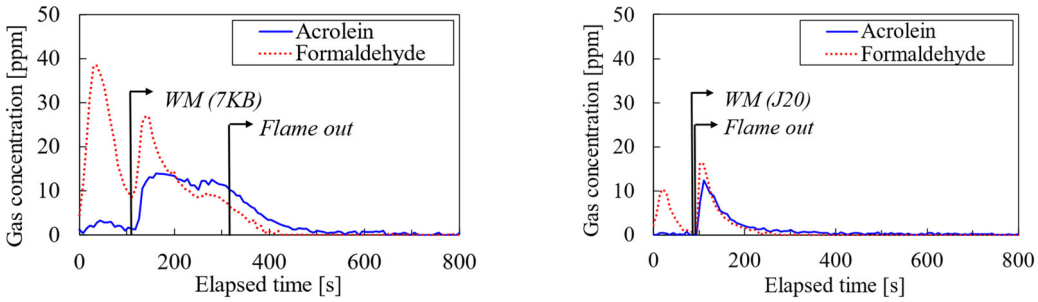

(a) Timber, Nozzle 7KB (b) Timber, Nozzle J20

Fig. 10. The concentrations of organic irritant gases.

concentration of CO increased to 411 ppm immediately after water-mist injection because of the flame expansion mechanism discussed earlier. The same trend of flame expansion was observed for PE and PU. With nozzle 7KB (Fig. 8(c)), on the other hand, the concentration of CO was detected slightly increased while CO_2 declined after water-mist application. Similar to timber combustion, reactions (2) and (3) occur to produce CO, but reaction (2) is limited in the maximum concentration as PP cannot generate char. In the case of PE, the slight but continuous production of CO and CO_2 occurred until an additional water supply completely put out the fire.

HCN concentration

The HCN concentration abruptly peaked at 18.5 ppm after the water mist was discharged on PE, as shown in Fig. 9(b). On the other hand, the experiment with the smaller-size water droplets by nozzle 7KB did not significantly display the production of HCN (Fig. 9(a)).

The sharp HCN peak observed with nozzle J20 appears similar to the sharp temperature increase in Fig. 5(b). Therefore, the flame-expansion phenomenon may be responsible for detecting HCN in the case of PE. As PE does not contain the N element, the HCN production should be associated with reactions involving atmospheric nitrogen. According to previous research [24], HCN is formed by the reaction (4) with thermal NO_x. The flame-expansion phenomenon that occurs only with nozzle J20 enhances the production of thermal NO_x, leading to the production of HCN.

$$C_iH_j + NO \rightarrow HCN \rightarrow NH \rightarrow N \rightarrow N_2 \quad (4)$$

With PU, which contains the N element, the HCN concentration increased at the beginning before the water mist was discharged (both nozzles), as shown in Figs. 9(c) and 9(d). After the water-mist injection, the maximum HCN concentration increased to 26.5 ppm when

Table 6. Overall factors affecting combustion behavior and toxic-gas production.

Polymers	Timber	PP	PE	PMMA	PS	PU
Chemical and physical properties						
Natural polymers	✓					
Thermoplastics		✓	✓	✓		
Thermosets					✓	✓
Char and/or surface products	✓			✓	✓	✓
Nitrogen-containing						✓
Burning characteristics						
Flame expansion		✓	✓			✓
Toxic-gas production						
CO and CO_2	✓	✓	✓	✓	✓	✓
Delayed CO reduction after small water-droplet application	✓			✓		✓
HCN		✓	✓			✓
Formaldehyde and acrolein	✓					
Sudden increase after large water-droplet application		✓	✓			✓

nozzle J20 was used. The flame-expansion phenomenon caused the increased HCN level.

Formaldehyde and acrolein concentrations

Fig. 10 shows that in addition to CO and CO_2, formaldehyde (CH_2O) and acrolein (C_3H_4O) (organic irritant gases) were also formed from the combustion of timber. The evolution of formaldehyde is similar to that of CO, affected by incomplete combustion. On the other hand, the concentration of acrolein was minor in the initial stage of the combustion. The production of formaldehyde and acrolein rose as the water was supplied and gradually decreased to negligible levels.

Table 6 summarizes the factors that affect toxic-gas production. The influences of the type of polymer on toxic gas evolution are explicated. Because of reaction (2), char-forming materials produce a high CO level during water-mist suppression. The char layer also acts as insulation, reducing the cooling effect of water mist; therefore, the CO concentration tends to maintain a high level after small water-droplet application. Materials that do not contain the N element may produce HCN via the flame-expansion phenomenon through the production of thermal NO_x. The flame-expansion phenomenon also causes a sudden increase in toxic gas production after water is discharged. Table 6 summarizes the factors that affect toxic-gas production. The influences of the type of polymer on toxic gas evolution are explicated. Because of reaction (2), char-forming materials produce a high CO level during water-mist suppression. The char layer also acts as insulation, reducing the cooling effect of water mist; therefore, the CO concentration tends to maintain a high level after small water-droplet application. Materials that do not contain the N element may produce HCN via the flame-expansion phenomenon through the production of thermal NO_x. The flame-expansion phenomenon also causes a sudden increase in toxic gas production after water is discharged.

Conclusions

Scaled-model experiments were conducted to understand the influence of water-mist application on its fire-extinguishing performance and the production of toxic gases for various polymers. The experimental conditions were determined based on a previously-proposed Froude-number scaling law extended by considering low drop Reynolds numbers. Burning and extinguishing processes of natural, thermoplastic, and thermosetting polymers are discussed. The following are the major conclusions of this study:

(1) The primary mechanism of fire extinction was the cooling effect. On the other hand, the secondary mechanism, the oxygen dilution effect, occurs when the droplets are small enough to evaporate quickly, promoting the smothering effect.

(2) The size of the water droplet influenced the production of toxic gases. In general, larger droplets can extinguish a fire in a shorter time; hence, toxic gas concentrations decrease more rapidly. However, the large droplets tend to cause the flame expansion phenomenon for thermoplastics by splashing molten polymer. This flame expansion phenomenon leads to a rapid increase in toxic-gas production rate. The flame expansion phenomenon also causes the formation of HCN via the reaction of thermal NO_x.

(3) The formation of a char layer tends to slow down the fire-extinguishing process, which causes continuous CO production after water is discharged.

(4) The formation of formaldehyde and acrolein was observed in timber combustion. The evolution of their concentrations was similar to CO.

The present scale-model experiments are to reproduce the specific prototype fires. Parameters such as the compartment size or water flux density will influence the results. Parametric studies are necessary for further understanding the influences of water-mist application on compartment fire developments.

Acknowledgment

One of the authors (NT) acknowledges the financial support as a scholarship from Mitsubishi Gas Chemical (MGC) Memorial Foundation. This work was supported in part by JSPS KAKENHI Grant Number JP21H04593.

References

[1] Rahman, R., Taib, N. A., Khusairy, M., Bakri, B., Taib, S., "Importance of sustainable polymers for modern society and development," in: Rahman, R. (Ed.), Advances in Sustainable Polymer Composites, Woodhead, 2020, pp. 1–35.

[2] Purser, D. "Assessment of hazards to occupants from smoke, toxic gases and heat," in: Hurley, M. et al. (Eds.), The SFPE Handbook of Fire Protection Engineering, Springer, 2016, pp. 2207–2302.

[3] Nishino, T. "Analysis of the arson fire in the 1st studio of Kyoto Animation on 18 July 2019," August 2, 2019 (referred from URL at https://www.dpri.kyoto-u.ac.jp/contents/wp-content/uploads/2019/08/Analysis-of-Kyoto-Animation-Arson-Fire_20190802-1.pdf).

[4] Fire and Disaster Management Agency. "Explosion and fire in Fushimi Ward, Kyoto City, Kyoto Prefecture," December 23, 2019 (referred from URL at https://www.fdma.go.jp/disaster/info/items/1912231340.pdf) (In Japanese).

[5] Yomiuri Online Newspaper. "36th person killed in KyoAni arson... No arrest insight for the suspect with burns all over his body," October 5, 2019 (referred from URL at https://web.archive.org/web/20211115124857/https://www.sankei.com/article/20191005-FET2RAALYFMONIZQBUMXKCSYFM/) (In Japanese).

[6] Liu, Z., Kim, A. K., "A review of water mist fire suppression systems—fundamental studies," Journal of Fire Protection Engineering 10: 32–50, 1999 (In Japanese).

[7] Qin, J., Chow, W. K., "Bench-scale tests on PMMA fires with water mist," Polymer Testing 24: 39–63, 2005.

[8] Yao, B., Cong, B. H., Qin, J., Chow, W. K. "Experimental study of suppressing poly (methyl methacrylate) fires using water mists," Fire Safety Journal 47: 32–39, 2014.

[9] Tanaka, F., Mizukami, W., Moinuddin, K., "Fire cooling performance by water sprays using medium and small-scale model experiments with scaling relaxation," Fire Safety Journal 112: 102965, 2020.

[10] National Research Institute of Fire and Disaster, "Water mist fire extinguishing and effective application method," National Research Institute of Fire and Disaster Report 59: 127–153, 2003.

[11] Zhao, X., Yoshioka, H., Noguchi, T., Fujimoto, S., Tanaike, Y., Hayakawa, T., Hase, Y., Naruse, T., "Fundamental study of gas toxicity with respect to fire stages," Fire Science and Technology 26(1): 11–24, 2017.

[12] Hietaniemi, J., Kallonen, R., Mikkola, E., "Burning characteristics of selected substances: influence of suppression with water," Fire and Materials 23: 149–169, 1999.

[13] Shelley, J., "Tenability analysis of television fires in a sprinkler protected compartment," Fire Engineering Research Report 04/3, 2004.

[14] Heskestad, G., "Scaling the interaction of water sprays and flames," Fire Safety Journal 32: 535–548, 2002.

[15] Jayaweera, T., Yu, H. "Scaling of fire cooling by water mist under low drop Reynolds number conditions," Fire Safety Journal 43: 63–70, 2008.

[16] Yu, Z. "Physical scaling of water mist suppression of wood cribs fires in enclosures," in: Fire Safety Science—Proceedings of the Eleventh International Symposium, 2014, pp. 1222–1235.

[17] Quintiere, J. G., Principles of Fire Behavior, 2nd ed., CRC Press, Florida, FL, USA, 2017.

[18] NFPA 750, Standard on Water Mist Fire Protection Systems, 2019.

[19] Ota, M., Omiya, Y., Matsuyama, K., Masaki, N., Yamaguchi, J. "A study on smoke behavior in a compartment with sprinkler system activation—full scale compartment test using wood crib as fuel—," The AIJ Journal of Technology and Design 20(45): 587–592, 2014.

[20] Qin, J., Yao, B., Chow, W. K., "Experimental study of suppressing cooking oil fire with water mist using a cone calorimeter," Hospitality Management 23: 545–556, 2004.

[21] Dietenberger, M. A., Hasburgh, L. E., "Wood products: thermal degradation and fire," Module in Materials Science and Materials Engineering, 1–7, 2016.

[22] Pitts, W., Johnson, E., Bryner, N., "Carbon monoxide formation in fires by high-temperature anaerobic wood pyrolysis," Twenty-Fifth Symposium (International) on Combustion, The Combustion Institute, 1455–1462. 1994.

[23] Morikawa, T., "Effects of water vapor on evolution of carbon monoxide in combustion and pyrolysis," Journal of Combustion Toxicology 9: 85–96, 1982.

[24] Dagaut, P., Glarborg, P., Alzueta, M., "The Oxidation of hydrogen cyanide and related chemistry," Progress in Energy and Combustion Science 34: 1–46, 2008.